Comparison of depth of focus enhancing pupil masks based on a signal-to-noise ratio criterion after the deconvolution

Frédéric Diaz, François Goudail, Brigitte Loiseau, Jean-Pierre Huignard

▶ **To cite this version:**

Frédéric Diaz, François Goudail, Brigitte Loiseau, Jean-Pierre Huignard. Comparison of depth of focus enhancing pupil masks based on a signal-to-noise ratio criterion after the deconvolution. Journal of the Optical Society of America. A Optics, Image Science, and Vision, 2010, 27 (10), pp.2123-2131. hal-00747081

HAL Id: hal-00747081

https://hal-iogs.archives-ouvertes.fr/hal-00747081

Submitted on 30 Oct 2012

HAL is a multi-disciplinary open access archive for the deposit and dissemination of scientific research documents, whether they are published or not. The documents may come from teaching and research institutions in France or abroad, or from public or private research centers.

L'archive ouverte pluridisciplinaire **HAL**, est destinée au dépôt et à la diffusion de documents scientifiques de niveau recherche, publiés ou non, émanant des établissements d'enseignement et de recherche français ou étrangers, des laboratoires publics ou privés.

Comparison of depth-of-focus-enhancing pupil masks based on a signal-to-noise-ratio criterion after deconvolution

Frédéric Diaz,[1,2,*] François Goudail,[2] Brigitte Loiseaux,[1] and Jean-Pierre Huignard[1]

[1]*Thales Research & Technology, 1 Avenue Augustin Fresnel, 91767 Palaiseau Cedex, France*
[2]*Laboratoire Charles Fabry de l'Institut d'Optique, CNRS, Université Paris-Sud, Campus Polytechnique, RD 128, 91127 Palaiseau Cedex, France*
**Corresponding author: frederic.diaz@thalesgroup.com*

Received April 15, 2010; revised July 26, 2010; accepted August 9, 2010;
posted August 9, 2010 (Doc. ID 126894); published September 8, 2010

We consider optimization of hybrid imaging systems including a pupil mask for enhancing the depth of field and a digital deconvolution step. In a previous paper [Opt. Lett. **34**, 2970 (2009)] we proposed an optimization criterion based on the signal-to-noise ratio of the restored image. We use this criterion in order to optimize different families of phase or amplitude masks and to compare them, on an objective basis, for different desired defocus ranges. We show that increasing the number of parameters of the masks allows one to obtain better performance. © 2010 Optical Society of America

OCIS codes: 110.7348, 110.4280, 110.4100, 100.1830.

1. INTRODUCTION

In traditional imaging systems, the optics and the post-processing are designed separately. The optics should thus provide images as good as possible, which involves high fabrication costs and/or poor compactness. In contrast, with hybrid imaging systems, the optics and the post-processing are designed together, which allows one to correct the defects of the optics by the post-processing and to simplify the post-processing by making the point spread function (PSF) of the optics insensitive to some aberrations. It is possible, for instance, to increase the depth of field by using a lens with a high axial chromatic aberration in order to obtain at least one sharp color plane of an RGB image [1] or using a lattice-focal lens [2].

Another way to increase the depth of field is to use a pupil mask, which makes the optical system almost insensitive to the defocus, and to restore the image thanks to a deconvolution. Other post-processing method could also be used, such as a maximum-entropy algorithm combined with a logarithmic asphere [3]. Such results can be used to correct the axial chromatic aberrations [4] or to free infrared cameras from thermal defocus [5].

Different types of masks have been proposed to enhance the depth of field, such as cubic [6], logarithmic [7], fractional-power [8], exponential [9], polynomial [10], and rational [11] phase masks. They depend on parameters that are optimized with respect to an aimed application. One of the key issues is to determine which type of mask performs better. For that purpose, one has first to choose a performance criterion. An intuitive one is the final image quality after the deconvolution step [12]. We recently analyzed a criterion based on the mean square error (MSE) [13] and showed that the optimal values of the mask parameters result from a trade-off between two antagonistic effects: the variation of the PSF with respect to the defocus, whereas the deconvolution filter is unique, and the noise enhancement due to deconvolution. The purpose of this paper is to use this MSE-based criterion to compare, on an objective basis, the performance of different pupil masks proposed in the literature.

This paper is organized as follows. In Section 2, we describe the chosen image quality criterion and present some important aspects of its implementation. In Section 3, we consider several families of phase masks proposed in the literature and discuss the optimal parameter values obtained through our quality criterion. In Section 4, we apply this criterion to the optimization of an amplitude mask. In Section 5, we use these results to compare the performance of these different masks. Finally, we present our conclusions in Section 6.

2. PROPOSED IMAGE QUALITY CRITERION

A. Choice of the Image Quality Criterion

Let us assume that we observe a scene $O(r)$ with a defocused linear optical system. The acquired signal is given by

$$I_\psi(r) = h_\psi(r) * O(r) + n(r), \tag{1}$$

where r denotes the spatial position, the symbol $*$ refers to the convolution operation, $n(r)$ is the measurement noise, and $h_\psi(r)$ is the PSF of the optical system for a given defocus ψ defined by

$$\psi = \frac{\pi R^2}{\lambda}\left(\frac{1}{d_O} + \frac{1}{d_I} - \frac{1}{f}\right), \tag{2}$$

with R being the radius of the aperture and f, d_O, and d_I being the focal length, the object distance, and the image sensor plane distance, respectively. In this paper, for sim-

 © 2010 Optical Society of America

plicity's sake, we shall assume that the defocus is constant on the whole scene. However, the method we describe is also valid for three-dimensional scenes where the distance of objects depends on their positions in the scene.

We assume that $n(r)$ and $O(r)$ are stationary random processes, and we denote by $S_{nn}(\nu)$ and $S_{OO}(\nu)$ their respective power spectral densities (PSDs). The amount of noise in the scene is quantified by the input SNR_{in} defined as

$$SNR_{in}(\mathrm{dB}) = 10\log_{10}\left[\int S_{OO}(\nu)\mathrm{d}\nu / \int S_{nn}(\nu)\mathrm{d}\nu\right], \quad (3)$$

where ν denotes the spatial frequency.

Our purpose is to obtain an estimate $\hat{O}(r)$ of $O(r)$ by post-processing the acquired data with a linear deconvolution filter $d(r)$:

$$\hat{O}_{\psi}(r) = d(r) * I_{\psi}(r). \quad (4)$$

Note that we assume that the deconvolution filter is unique and does not depend on the defocus. We thus consider systems in which an estimation of the defocus is not available. The quality of restoration will be evaluated by the MSE between the object and its estimation [13]:

$$\begin{aligned} MSE_{\psi} &= \langle|\hat{O}_{\psi}(r) - O(r)|^2\rangle \\ &= \int |\tilde{d}(\nu)\tilde{h}_{\psi}(\nu) - 1|^2 S_{OO}(\nu)\mathrm{d}\nu + \int |\tilde{d}(\nu)|^2 S_{nn}(\nu)\mathrm{d}\nu, \end{aligned} \quad (5)$$

where the symbol $\sim$ refers to the Fourier transform and $\langle\ \rangle$ denotes averaging. In Eq. (5), the MSE is a sum of two terms. The first one is due to the discrepancy between the deconvolution filter and the actual PSF, and the second one is due to the noise enhancement due to deconvolution. The performance of the system for the whole desired defocus range is estimated by calculating the MSE averaged over n_{MSE} defocus values uniformly distributed in the range $\psi_i \in [0, \psi_{\mathrm{defoc\ max}}]$:

$$MSE_{\mathrm{mean}} = \frac{1}{n_{\mathrm{MSE}}}\sum_{i=1}^{n_{\mathrm{MSE}}} MSE_{\psi_i}. \quad (6)$$

Finally, the image quality criterion is the restored image quality (RIQ) of the post-processed image defined as

$$RIQ_{\mathrm{mean}}(\mathrm{dB}) = 10\log_{10}\left[\int S_{OO}(\nu)\mathrm{d}\nu / MSE_{\mathrm{mean}}\right], \quad (7)$$

and we denote by RIQ_{ψ} the RIQ of an image at a given defocus:

$$RIQ_{\psi}(\mathrm{dB}) = 10\log_{10}\left[\int S_{OO}(\nu)\mathrm{d}\nu / MSE_{\psi}\right]. \quad (8)$$

B. Shift of the PSF with Respect to the Defocus

Depending on the application, one has to take into account that the phase masks used to extend the depth of field are known to have their PSFs shifted with the defocus. This is due to a linear term in the phase transfer function that varies with the defocus. Let us take as an example the cubic phase mask [6] whose transmittance is $t(x,y) = \exp[i\varphi_{\mathrm{cub}}(x,y)]$, with

$$\varphi_{\mathrm{cub}}(x,y) = \alpha_{\mathrm{cub}}(x^3 + y^3), \quad (9)$$

with x and y being the coordinates of the pupil, normalized to 1, and α_{cub} being the mask parameter. To illustrate the translation occurring with the defocus, let us write the phase excursion due to the mask and the defocus of magnitude ψ if α_{cub} is nonzero:

$$\begin{aligned} \varphi_{\mathrm{tot}}(x,y) &= \varphi_{\mathrm{cub}}(x,y) + \psi(x^2 + y^2) \\ &= \alpha_{\mathrm{cub}}\left(x - \frac{\psi}{3\alpha_{\mathrm{cub}}}\right)^3 + \alpha_{\mathrm{cub}}\left(y - \frac{\psi}{3\alpha_{\mathrm{cub}}}\right)^3 - \frac{\psi^2(x+y)}{3\alpha_{\mathrm{cub}}} \\ &\quad - \frac{2\psi^3}{81{\alpha_{\mathrm{cub}}}^2}. \end{aligned} \quad (10)$$

The first two terms induce a slight deformation of the shape of the PSF, whereas the fourth one is a constant phase factor that has no influence. The third term is a linear phase that corresponds to a translation of the PSF equal to $\delta x = -(f\psi^2)/(3\alpha_{\mathrm{cub}}kR)$.

Such a translation of the PSF with the defocus is also present in the other types of phase masks considered in this paper. Unfortunately, it generally cannot be as easily calculated as in the case of the cubic phase mask, and it must be estimated numerically. Indeed, we consider applications where a slight global translation does not affect the image quality and consequently must have no effect on the MSE. For that purpose, to compute the MSE, we have to consider a non-translated version of the PSF that we denote by h^c_{ψ}. For any value of ψ, h^c_{ψ} is centered at the same location as for $\psi = 0$. The translation δx between h_0 and h_{ψ} is estimated by minimizing the following MSE with respect to δx:

$$MSE_{\mathrm{translat}}(\delta x) = \langle|\tilde{h}_0(\nu) - \tilde{h}_{\psi}(\nu)\exp(-2i\pi\nu\delta x)|^2\rangle. \quad (11)$$

One obtains an estimate of the translation as

$$\delta\hat{x} = \arg\min_{\delta x}[MSE_{\mathrm{translat}}(\delta x)],$$

and the transfer function of the centered mask is estimated as

$$\tilde{h}^c_{\psi}(\nu) = \tilde{h}_{\psi}(\nu)\exp(-2i\pi\nu\delta\hat{x}). \quad (12)$$

The MSE_{ψ} expression in Eq. (6) can then be replaced with

$$MSE_{\psi} = \int |\tilde{d}(\nu)\tilde{h}^c_{\psi}(\nu) - 1|^2 S_{OO}(\nu)\mathrm{d}\nu + \int |\tilde{d}(\nu)|^2 S_{nn}(\nu)\mathrm{d}\nu. \quad (13)$$

C. Deconvolution Filter

In order to obtain the best performance with a given optical system, it was shown that the deconvolution filter that minimizes the averaged MSE in Eq. (13) is [13]

$$\tilde{d}(\nu) = \frac{\frac{1}{n_d}\sum_{i=1}^{n_d} \tilde{h}^{c^*}_{\psi_i}(\nu)}{\frac{1}{n_d}\sum_{i=1}^{n_d} |\tilde{h}^{c}_{\psi_i}(\nu)|^2 + \frac{S_{nn}(\nu)}{S_{OO}(\nu)}}. \quad (14)$$

It is calculated by taking $n_d < n_{\mathrm{MSE}}$ defocus values uniformly distributed in the range $\psi_i \in [0, \psi_{\mathrm{defoc\ max}}]$. This filter depends not only on the PSD of the sensor noise, which is considered to be known, but also on the PSD of the object which is generally unknown. In this paper, we shall consider two cases. In the first one, the perfect image is assumed to be known and the object PSD is taken as the square of its Fourier transform: $S_{OO}(\nu) = |\tilde{O}(\nu)|^2$. This method will be called the *ideal filter* in the following. In the second case, we will use a generic model for the object PSD. Models for the power spectrum of natural images have been proposed [14]. In this paper, an estimate of $S_{OO}(\nu)$ was generated by averaging the PSD of images of different types. We will call this second method the *generic filter*.

3. OPTIMIZATION OF PHASE MASK PARAMETERS

In this section, we consider different types of phase masks proposed in the literature. Our purpose is to determine the optimal values of their parameters and their performance as functions of the desired depth of focus. The image quality defined in the previous section depends on parameters such as the level of detector noise, the desired depth of field, and the profile of the phase mask. We consider two types of scenes: a spoke target that contains high spatial frequencies and the classical "Lena" image that contains mostly low spatial frequencies (see Fig. 1). The input signal-to-noise ratio, SNR_{in}, is set to 34 dB. The noise is a Gaussian white noise, but we have checked that comparable results are obtained with a signal dependent noise such as shot noise. We first consider that the maximal expected defocus value $\psi_{\mathrm{defoc\ max}}$ is 15.75 and take $n_d = 5$ defocus values to compute the deconvolution filter and $n_{\mathrm{MSE}} = 11$ defocus values to estimate MSE_{mean}. Both ideal and generic filters will be used to recover the image.

A. Cubic Phase Mask

The cubic phase mask was proposed by Dowski and Cathey [6] in 1995. They searched for the monomial phase function of the type $\varphi_{\mathrm{cub}}(x) = \alpha_{\mathrm{cub}} x^{\gamma}$ that minimizes the variation of the optical transfer function (OTF) with misfocus. They found that the optimal exponent for that purpose is $\gamma = 3$. In two dimensions, the phase function of the cubic mask is given by Eq. (9). This mask depends on a single parameter α_{cub} that represents the depth of the phase modulation.

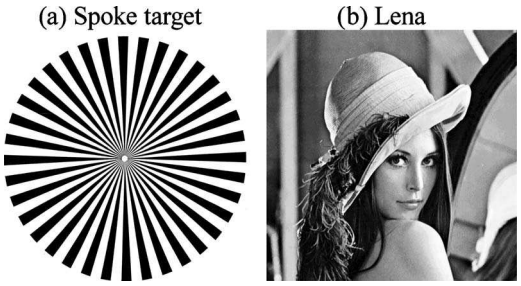

Fig. 1. Objects used to optimize the different masks.

RIQ_{mean} as a function of α_{cub} is displayed in Fig. 2 for the spoke target and Lena, using either the ideal deconvolution filter or the generic one. For low values of α_{cub}, the PSF is too sensitive to the defocus. For high values of α_{cub}, the noise is enhanced by the deconvolution filter. The optimal parameter $\alpha_{\mathrm{cub,opt}}$ is thus a compromise between these two antagonistic effects. It does not depend on the object or on the used deconvolution filter, and is equal to $\alpha_{\mathrm{cub,opt}} = 15.74$ rad in these conditions, leading to $RIQ_{\mathrm{mean}} = 12.14$ dB for the spoke target and $RIQ_{\mathrm{mean}} = 16.01$ dB for Lena with the ideal filter. The better results obtained with Lena are due to its low spatial frequency content, and the better results obtained with the ideal filter are due to better adequacy between the filter and the object.

The optimal value $\alpha_{\mathrm{cub,opt}}$ tends to increase with $\psi_{\mathrm{defoc\ max}}$ (Fig. 3). This is easily understandable since the larger is the desired depth of field, the more insensitive the PSF of the optical system needs to be. It is also noted that the value of $\alpha_{\mathrm{cub,opt}}$ is almost independent of the object and of the deconvolution filter.

B. Logarithmic Phase Mask

The logarithmic phase mask was introduced by Sherif *et al.* [7]. This phase mask was designed to make the PSF insensitive to the defocus. The expression of the logarithmic phase mask is

$$\varphi_{\log}(x,y) = \alpha_{\log}\,\mathrm{sgn}(x)x^2\,\log(|x| + \beta_{\log}) + \alpha_{\log}\,\mathrm{sgn}(y)y^2\,\log(|y| + \beta_{\log}),$$

with $\alpha_{\log}$ and $\beta_{\log}$ being the mask parameters.

The optimal parameters are $\alpha_{\log,\mathrm{opt}} = 26.43$ rad and $\beta_{\log,\mathrm{opt}} = 0.63$, leading to $RIQ_{\mathrm{mean}} = 12.05$ dB for the spoke target and ideal deconvolution filter (Fig. 4). With such optimal parameters, it appears that the difference between the cubic and logarithmic phase functions is almost a linear term $\varphi_{\mathrm{tilt}}(x,y) = 2.625(x+y)$. By subtracting this linear term from the logarithmic phase function, the difference between the cubic and logarithmic phase functions is inferior to 0.4 rad with a standard deviation infe-

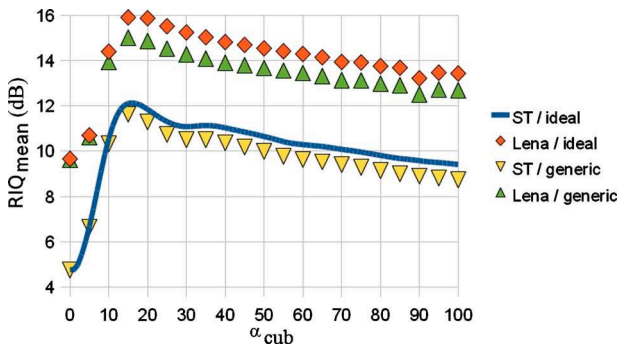

Fig. 2. (Color online) RIQ_{mean} as a function of α_{cub} for the spoke target and Lena, with $\psi_{\mathrm{defoc\ max}} = 15.75$, using either the ideal filter or the generic one.

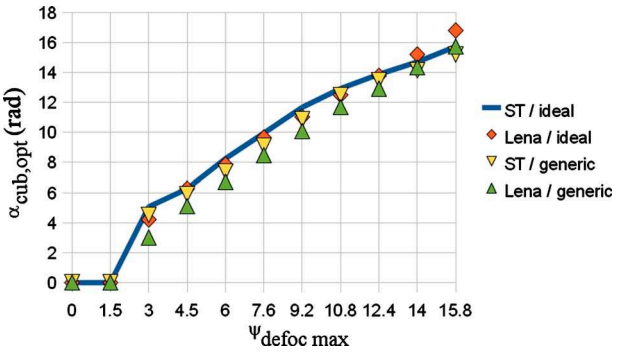

Fig. 3. (Color online) Optimal cubic phase mask parameter $\alpha_{cub,opt}$ as a function of the desired depth of field.

rior to 0.22 rad. Figure 5 shows the profiles of the cubic and logarithmic functions with the subtracted tilt. As both the logarithmic and cubic phase masks have been calculated to ensure an insensitivity of the response of the optical system to the defocus (OTF for the cubic phase mask and PSF for the logarithmic phase mask), the fact that they have equivalent performance is thus coherent with the criteria from which they have been derived. As with the cubic phase mask parameter, the optimal parameters of the logarithmic phase mask increase with the desired depth of field (Fig. 6) and are almost the same whatever is the object or the deconvolution filter.

C. Fractional-Power Phase Mask

As phase functions $\varphi(x)=\alpha x^n$, with $n=0,1,2,3,4,\ldots$, are well-known (plane surface for $n=0$, prism for $n=1$, lens for $n=2$, cubic phase mask for $n=3$, and lens with spherical aberration for $n=4$), Sauceda and Ojeda-Castañeda considered phase functions $\varphi(x)=\alpha x^{n+\varepsilon}$, with $0\le\varepsilon<1$ [8]. The expression of their fractional-power phase mask is

$$\varphi_{frac}(x,y)=\alpha_{frac}(\mathrm{sgn}(x)|x|^{\beta_{frac}}+\mathrm{sgn}(y)|y|^{\beta_{frac}}).$$

A fractional-power phase mask with $\beta_{frac}=3$ corresponds to the cubic phase mask so that we expect to improve the performance with the fractional-power phase mask compared to the cubic phase mask.

The optimal parameters are $\alpha_{frac,opt}=19.87$ rad and $\beta_{frac,opt}=3.49$, leading to $RIQ_{mean}=12.75$ dB for the spoke target and ideal deconvolution filter (Fig. 7). The performance is better when $\beta_{frac}\ge 3$. In contrast, for $\beta_{frac}\approx 2$, the performance is poor, as the phase mask corresponds to a simple defocus.

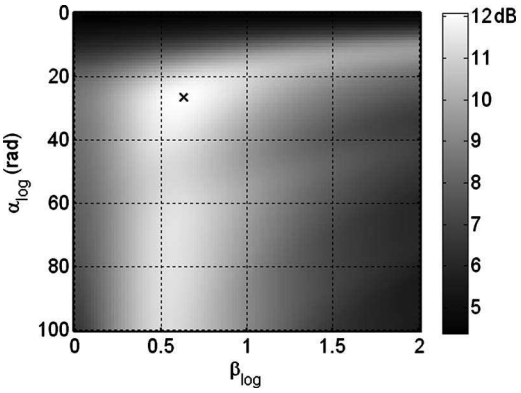

Fig. 4. RIQ_{mean} as a function of the logarithmic phase mask parameters α_{log} and β_{log}, for the spoke target and ideal deconvolution filter, with $\psi_{defoc\ max}=15.75$.

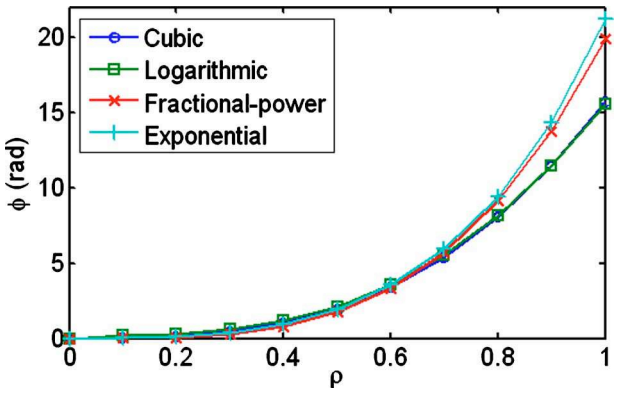

Fig. 5. (Color online) Profile along the x direction of the different phase masks with their optimal parameters.

Because $\beta_{frac,opt}$ is close to 3, the shape of the fractional-power phase mask is still very close to the shape of the cubic phase mask near the origin. The difference becomes significant only for $\sqrt{x^2+y^2}\ge 0.68$ (Fig. 5).

When $\psi_{defoc\ max}$ increases, the optimal exponent $\beta_{frac,opt}$ tends to 3, which corresponds to a cubic phase mask (Fig. 8). This is understandable since when the desired depth of focus increases, the response of the optical system needs to be more invariant to the defocus, which is precisely what the cubic phase mask is optimized for.

D. Exponential Phase Mask

The exponential phase mask was suggested by Yang *et al.* [9] in 2007, in order to obtain a mask more flexible than the cubic one thanks to its two parameters instead of a single one. The phase function of the exponential phase mask is

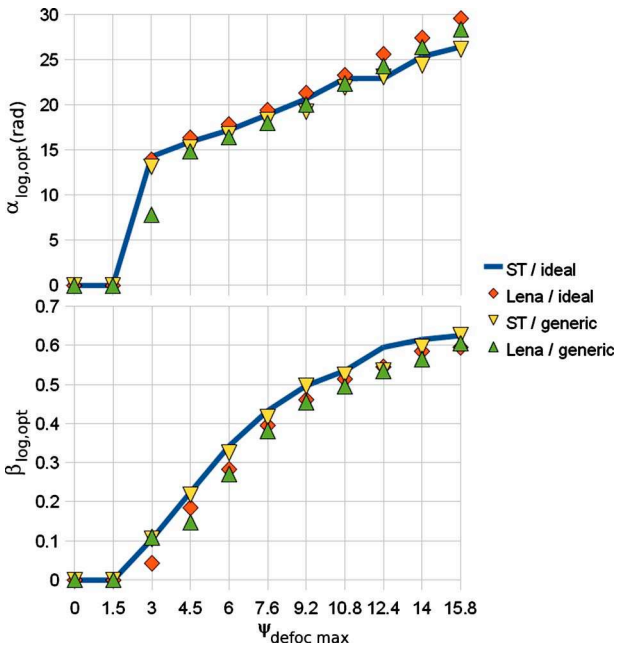

Fig. 6. (Color online) Optimal logarithmic phase mask parameters $\alpha_{log,opt}$ and $\beta_{log,opt}$ as functions of the desired depth of field.

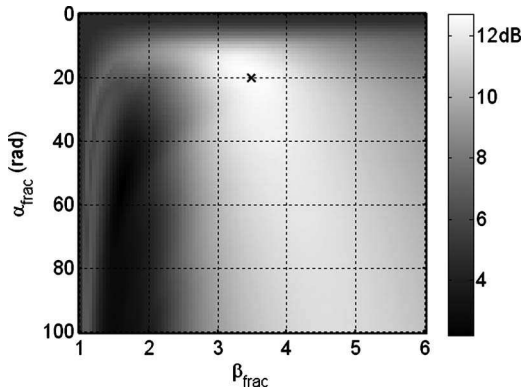

Fig. 7. RIQ_{mean} as a function of the fractional-power phase mask parameters, for the spoke target and ideal deconvolution filter, with $\psi_{defoc\ max}=15.75$.

$$\varphi_{exp}(x,y) = \alpha_{exp}x[\exp(\beta_{exp}x^2) - 1] + \alpha_{exp}y[\exp(\beta_{exp}y^2) - 1].$$

At low values of β, it can be approximated by

$$\varphi_{exp}(x,y) = \alpha_{exp}\beta_{exp}(x^3 + y^3) + \alpha_{exp}{\beta_{exp}}^2(x^5 + y^5)/2,$$

and at very low values of β, the exponential phase mask is thus equivalent to a cubic phase mask with a parameter $\alpha_{cub}=\alpha_{exp}\beta_{exp}$. Its optimal performance should thus be at least as good as that of the cubic phase mask.

The optimal parameters are $\alpha_{exp,opt}=19.38$ rad and $\beta_{exp,opt}=0.74$, leading to $RIQ_{mean}=13.1$ dB, for the spoke target and the ideal filter (Fig. 9), which is close to RIQ_{mean} obtained with the optimal fractional-power phase mask. It can be seen in Fig. 5 that the two masks are indeed very close, as the difference between them does not exceed 0.5 rad over 90% of their surfaces, and 1.37 rad on the whole surface.

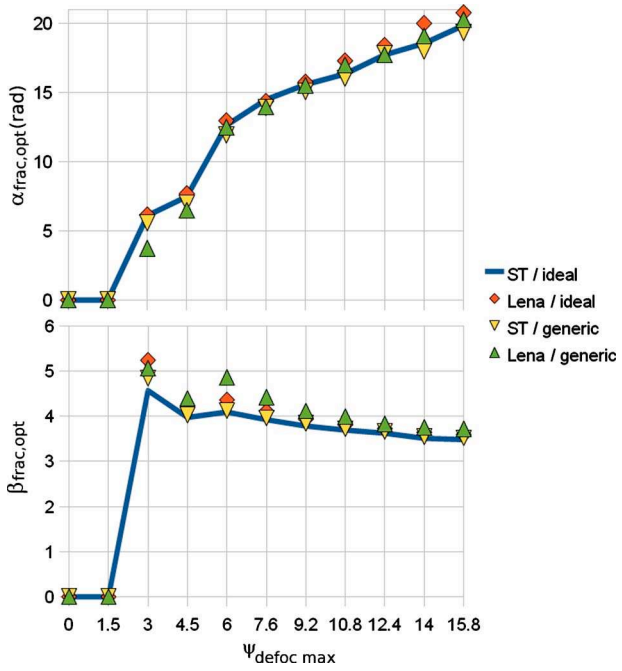

Fig. 8. (Color online) Optimal fractional-power phase mask parameters $\alpha_{frac,opt}$ and $\beta_{frac,opt}$ as functions of the desired depth of field.

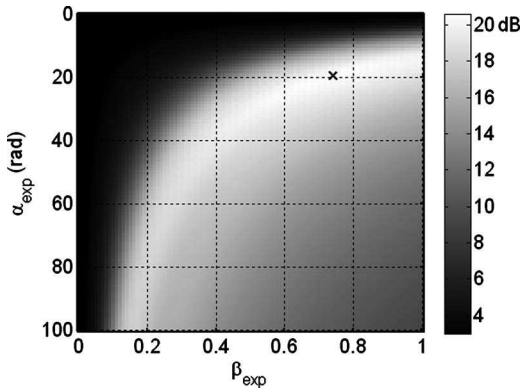

Fig. 9. RIQ_{mean} as a function of the exponential phase mask parameters, for the spoke target and ideal deconvolution filter, with $\psi_{defoc\ max}=15.75$.

The RIQ remains almost equal for parameter sets where the product $\alpha_{exp}\beta_{exp}$, which corresponds to the coefficient of the cubic term α_{cub} in Eq. (9), is constant. The optimal parameters $\alpha_{exp,opt}$ and $\beta_{exp,opt}$ correspond to a coefficient of the cubic term equal to $\alpha_{exp}\beta_{exp}=14.34$ rad, which is slightly lower than the optimal cubic mask parameter $\alpha_{cub,opt}=15.74$ rad.

When $\psi_{defoc\ max}$ increases, $\beta_{exp,opt}$ is getting smaller (Fig. 10), which means that the exponential phase mask also tends to be a cubic phase mask. The variations of the optimal parameters with $\psi_{defoc\ max}$ are quite chaotic. However, their product $\alpha_{exp}\beta_{exp}$, corresponding to the coefficient of the cubic term of Eq. (8), increases smoothly with $\psi_{defoc\ max}$, as well as the product $\alpha_{exp}{\beta_{exp}}^2/2$ that corresponds to the coefficient of the fifth order term (Fig. 11).

4. OPTIMIZATION OF A BINARY AMPLITUDE MASK

One of the advantages of the proposed image quality criterion is to make it possible to compare the performances

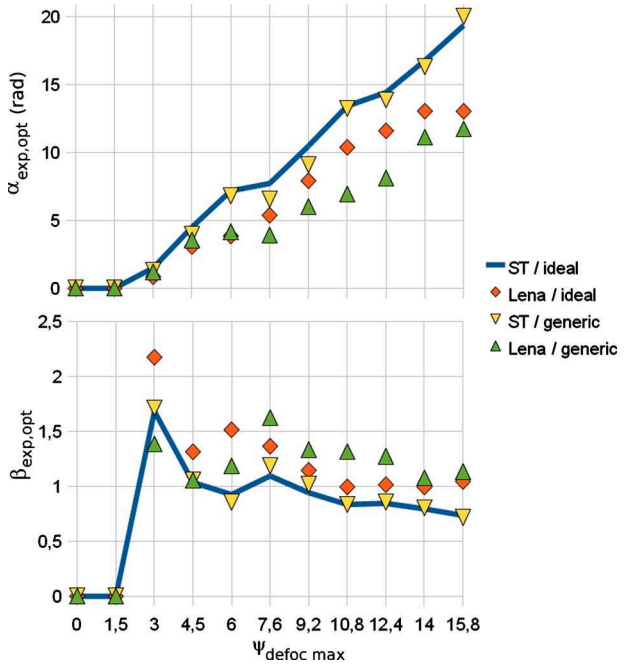

Fig. 10. (Color online) Optimal exponential phase mask parameters $\alpha_{exp,opt}$ and $\beta_{exp,opt}$ as functions of the desired depth of field.

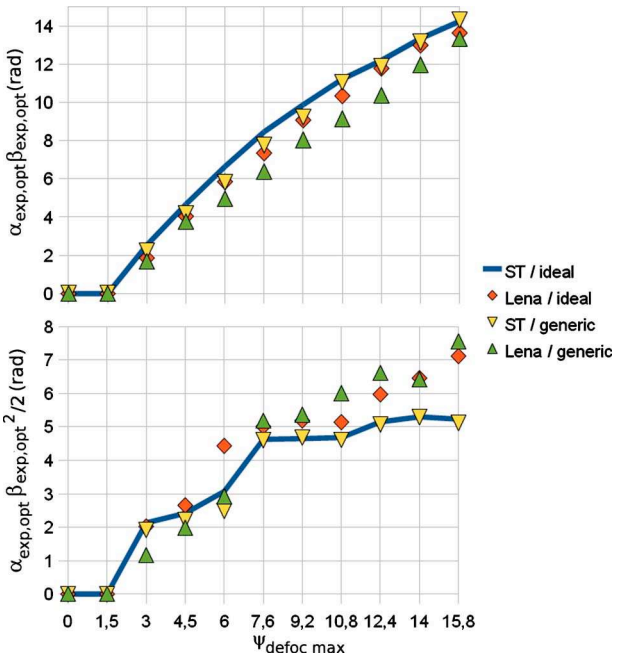

Fig. 11. (Color online) Optimal exponential phase mask parameters $\alpha_{exp,opt}\beta_{exp,opt}$ and $\alpha_{exp,opt}\beta_{exp,opt}^2/2$ as functions of the desired depth of field.

of masks of different characteristics. We will consider in this section the performance obtained with the well-known circular amplitude apodizer whose transmittance is

$$A(x,y) = 1 \quad \text{if } 0 \le \sqrt{x^2+y^2} \le \alpha_{amp} \le 1$$

$$= 0 \quad \text{otherwise},$$

which corresponds to a lens whose aperture can be adjusted.

The optimal parameter is $\alpha_{amp,opt}=0.42$, leading to $RIQ_{mean}=10.55$ dB, for the spoke target and the ideal deconvolution filter (Fig. 12). The same optimal parameter is obtained with the image Lena, leading to $RIQ_{mean}=15.3$ dB. So RIQ_{mean} remains significantly below that obtained with any of the pure phase masks considered in the previous section. To further interpret this result, let us notice that reducing the aperture size R of the lens by a factor of $1/0.42=2.4$ corresponds to a reduction in the defocus parameter ψ by a factor of $2.4^2=5.7$ [see Eq. (2)]:

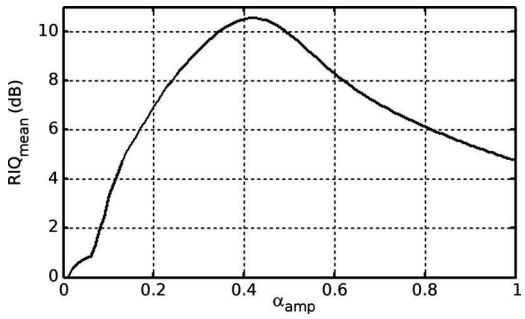

Fig. 12. RIQ_{mean} as a function of the amplitude mask parameter for the spoke target and ideal deconvolution filter, with $\psi_{defoc\ max}=15.75$.

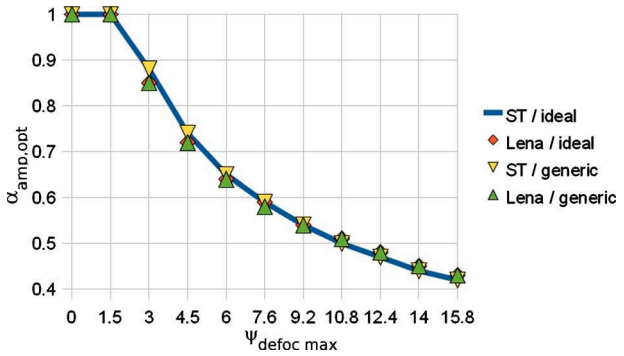

Fig. 13. (Color online) Optimal amplitude mask parameter as a function of the desired depth of field.

the maximal defocus thus decreases from $\psi=15.75$ to $\psi=2.78$. This value is coherent with the fact that a simple lens without mask or post-processing is thought to achieve a good image quality for $\psi \in [0, 2.5]$. As the desired depth of field increases, the aperture is reduced (Fig. 13). However, shrinking the aperture reduces the transverse resolution by a factor of 2.4 and the transmitted energy by a factor of 5.7. Figure 14 shows the lower transverse resolution of the image without deconvolution, where the center of the spoke target is blurred. At the same time, the loss of transmitted energy makes the noise more visible. The deconvolution step makes the image sharper but cannot recover the spatial frequency content of the object that has been lost because of the aperture reduction. This is why the center of the spoke target remains blurred. This blur is less visible on Lena as it has mainly low spatial frequency content.

This result tends to prove that pure phase masks are more suitable to enhance the depth of field than pure amplitude masks. We have also considered the annular aperture in order to obtain the following transmittance:

$$A(x,y) = 1 \quad \text{if } 0 \le \beta_{amp} \le \sqrt{x^2+y^2} \le \alpha_{amp} \le 1$$

$$= 0 \quad \text{otherwise},$$

but it does not allow one to increase the performance: the optimal RIQ is practically the same as the RIQ when β_{amp}

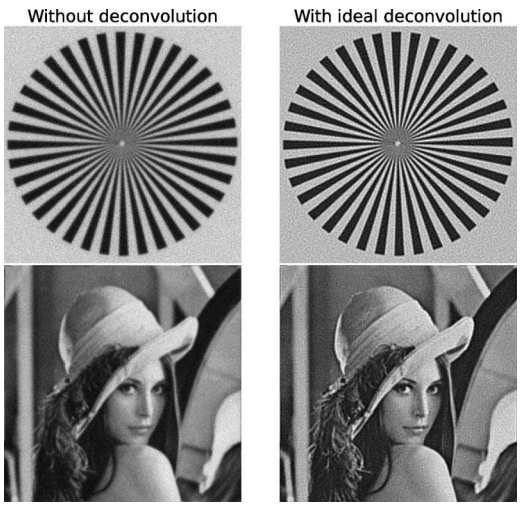

Fig. 14. Images obtained with the amplitude mask, at the focal plane, with $\psi_{defoc\ max}=15.75$.

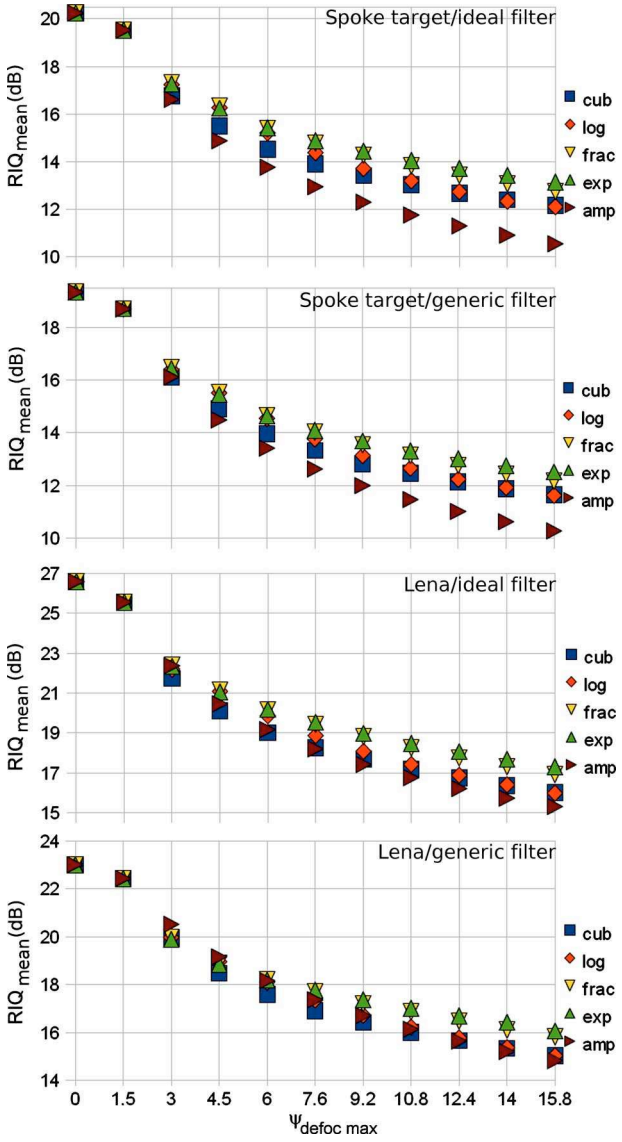

Fig. 15. (Color online) RIQ_{mean} obtained with the different phase masks for the spoke target and Lena using either their ideal or the generic deconvolution filter.

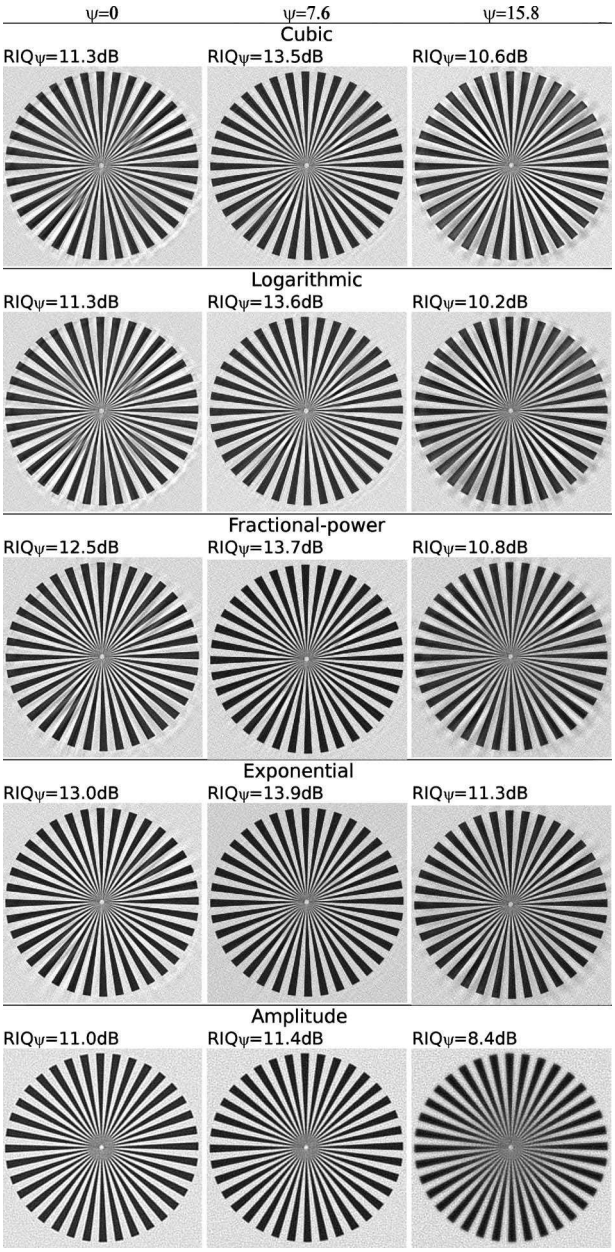

Fig. 16. Images of the spoke target obtained at different defocus values with the different masks using their optimal parameters and the ideal deconvolution filter, with $\psi_{\text{defoc max}} = 15.75$.

is equal to zero. Finally, we tried to combine the aperture reduction with a cubic phase function, but the optimal configuration always led to a full size aperture. It thus seems that when using deconvolution, it is useless to add a binary amplitude modulation to a phase mask.

5. DISCUSSION ON THE PERFORMANCE

The restored image quality (RIQ_{mean}) obtained with the optimal parameter values was used as the objective criterion to evaluate the performance of different masks. In this section, the performance of the four phase masks considered in Section 3 and the amplitude mask considered in Section 4 will be compared on this basis.

Let us first consider again Fig. 5, which presents the profiles in the x direction of the considered phase masks with optimal parameters. Two groups of masks clearly appear: on one side, the cubic and logarithmic masks, and on the other side the fractional-power and exponential masks. This explains the comparable performance inside each group. The RIQ obtained with the different masks as a function of the desired depth of focus is displayed in Fig. 15. The cubic phase mask presents a slight advantage for a large depth of field, while the logarithmic phase mask is better for a moderate depth of field. The fractional-power and exponential phase masks perform significantly better than the two others, which is understandable since both have two free parameters instead of one. Regarding the type of deconvolution filter, it can be stated that using the generic filter decreases the RIQ by about 1 dB, but the ranking of the mask performances remains the same.

The performance of the amplitude mask is significantly lower than those of the phase masks with the spoke target containing high spatial frequencies, as the cutoff fre-

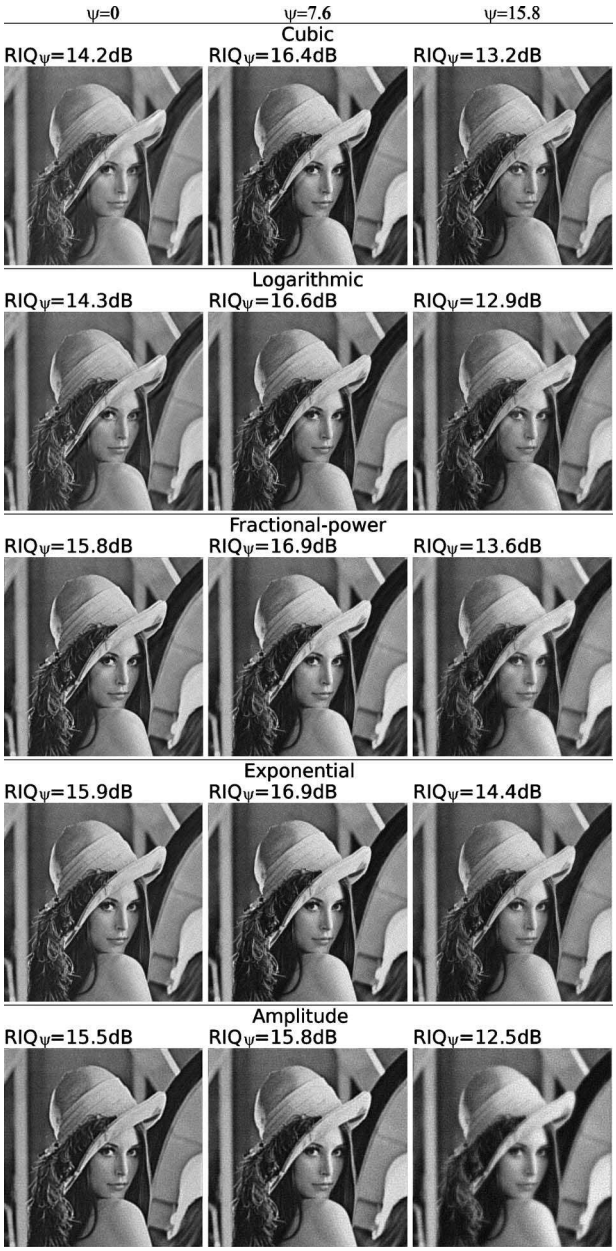

Fig. 17. Images of Lena obtained at different defocus values with the different masks using their optimal parameters and the generic deconvolution filter, with $\psi_{\text{defoc max}}=15.75$.

quency of the optics is decreased. As Lena contains mostly low spatial frequencies, this loss of resolution has less influence on the RIQ.

It is verified in Fig. 16 where are presented the images obtained with the different masks that the results are better with the fractional-power and exponential phase masks than with the cubic and the logarithmic ones. Indeed, the restored image of the spoke target has fewer artifacts with the exponential phase mask than with the cubic phase mask. In order to reduce these artifacts, one could try to use a higher value of α_{cub}, but this would lead to a noisier result. The performance of the binary amplitude mask is poor at large defocus values. The image of the spoke target is blurred at $\psi=15.75$, and the corresponding RIQ is low compared to what is obtained with the other phase masks. The visual perception of the image thus confirms the relevance of the chosen RIQ criterion. This result also tends to prove that phase masks are more suitable to enhance the depth of field than amplitude masks.

The same conclusions will be reached with Lena and generic deconvolution filter (Fig. 17). We observe more artifacts with the cubic and logarithmic phase masks than with the fractional-power and the exponential phase masks, especially in the region of the edge of her hat, and the amplitude mask still gives a blurred image at $\psi=15.75$.

6. CONCLUSION

We used an optimization criterion that takes into account the non-invariance of the PSF and the noise enhancement induced by the deconvolution process. This criterion allowed us to characterize the performance of several phase masks found in the literature and to compare them. It appears that all these masks are suitable for enhancing the depth of field and are more appropriate than a binary amplitude mask. Fractional-power and exponential phase masks have one more parameter that makes it possible to improve their performances compared to the cubic and logarithmic phase masks.

Of course, these conclusions are limited to the considered application, which was image restoration using deconvolution. If other applications are considered, such as parameter estimation [15], the quality criterion to use is different and so could be the conclusions and the ranking of the different types of masks. Furthermore, the present analysis is limited to small angle properties of optical systems, and an interesting prospect is to extend it to more realistic imaging systems featuring field varying aberrations.

REFERENCES

1. C.-L. Tisse, H. Nguyen, R. Tessieres, M. Pyanet, and F. Guichard, "Extended depth-of-field using sharpness transport across colour channels," Proc. SPIE **7061**, 706105 (2008).
2. A. Levin, "4-D frequency analysis of computational cameras for depth of field extension," in *Frontiers in Optics*, OSA Technical Digest (2009), paper FThX1.
3. W. Chi and N. Georges, "Computational imaging with the logarithmic asphere: theory," J. Opt. Soc. Am. A **20**, 2260–2273 (2003).
4. H. Wach, E. Dowski, and T. Cathey, "Control of chromatic focal shift through wave-front coding," Appl. Opt. **37**, 5359–5367 (1998).
5. E. Dowski, R. Cormack, and S. Sarama, "Wavefront coding: jointly optimized optical and digital imaging systems," Proc. SPIE **4041**, 114–120 (2000).
6. E. Dowski and T. Cathey, "Extended depth of field through wave-front coding," Appl. Opt. **34**, 1859–1866 (1995).
7. S. Sherif, T. Cathey, and E. Dowski, "Phase plate to extend the depth of field of incoherent hybrid imaging systems," Appl. Opt. **43**, 2709–2721 (2004).
8. A. Sauceda and J. Ojeda-Castañeda, "High focal depth with fractional-power wave fronts," Opt. Lett. **29**, 560–562 (2004).
9. Q. Yang, L. Liu, and J. Sun, "Optimized phase pupil masks for extended depth of field," Opt. Commun. **272**, 56–66 (2007).

10. N. Caron and Y. Sheng, "Polynomial phase masks for extending the depth of field of a microscope," Appl. Opt. **47**, E39–E43 (2008).
11. F. Zhou, G. Li, H. Zhang, and D. Wang, "Rational phase mask to extend the depth of field in optical-digital hybrid imaging systems," Opt. Lett. **34**, 380–382 (2009).
12. D. Stork and D. Robinson, "Theoretical foundations for joint digital-optical analysis of electro-optical imaging systems," Appl. Opt. **47**, B64–B75 (2008).
13. F. Diaz, F. Goudail, B. Loiseaux, and J.-P. Huignard, "Increase in depth of field taking into account deconvolution by optimization of pupil mask," Opt. Lett. **34**, 2970–2972 (2009).
14. R. Balboa and N. Grzywacz, "Power spectra and distribution of contrasts of natural images from different habitats," Vision Res. **43**, 2527–2537 (2003).
15. R. Narayanswamy, G. Johnson, P. Silveira, and H. Wach, "Extending the imaging volume for biometric iris recognition," Appl. Opt. **44**, 701–712 (2005).